Talanta 80 (2009) 656–663

Contents lists available at ScienceDirect

Talanta

journal homepage: www.elsevier.com/locate/talanta

Differential pulse voltammetric simultaneous determination of noradrenalin and acetaminophen using a hematoxylin biosensor

Navid Nasirizadeh, Hamid R. Zare*

Department of Chemistry, Yazd University, P.O. Box 89195-741, Yazd 89195-741, Iran

ARTICLE INFO

Article history:
Received 21 April 2009
Received in revised form 20 July 2009
Accepted 22 July 2009
Available online 30 July 2009

Keywords:
Noradrenalin
Acetaminophen
Differential pulse voltammetry
Biosensor
Hematoxylin

ABSTRACT

A highly efficient noradrenalin (NA) biosensor was fabricated on the basis of hematoxylin electrodeposited on a glassy carbon electrode, GCE. The cyclic voltammetric responses of the hematoxylin biosensor at various scan rates, which were obtained in a 0.25 mmol L^{-1} NA solution, showed the characteristic shape typical of an EC_{cat} process. The kinetic parameters such as electron transfer coefficient, α, the catalytic electron transfer rate constant, k', and the standard catalytic electron transfer rate constant, k^0, for oxidation of NA at the hematoxylin biosensor surface were estimated using cyclic and RDE voltammetry. The peaks of differential pulse voltammetric (DPV) for NA and acetaminophen (AC) oxidation at the hematoxylin biosensor surface were clearly separated from each other when they co-exited in the physiological pH (pH 7.0). It was, therefore, possible to simultaneously determine NA and AC in the samples at a hematoxylin biosensor. Linear calibration curves were obtained for 5.0×10^{-1} to 65.40 μmol L^{-1} and 65.40–274.20 μmol L^{-1} of NA, and for 12.00–59.10 μmol L^{-1} and 59.10–261.70 μmol L^{-1} of AC. The sensitivities of the biosensor to NA in the absence and presence of AC were found virtually the same, which indicates the fact that the electrocatalytic oxidation processes of NA are independent of AC and, therefore, simultaneous or independent measurements of the two analytes (NA and AC) are possible without any interference. The results of 16 successive measurements show an average voltammetric peak current of 1.13 ± 0.03 μA for an electrolyte solution containing 5.00 μmol L^{-1} NA. The hematoxylin biosensor has been satisfactorily used for the determination of NA and AC in pharmaceutical formulations. The results obtained, using the biosensor, are in very good agreement with those declared in the label of pharmaceutical inhalation products.

1. Introduction

The chemical modifications of bare electrodes with a thin film of a suitable electroactive species offer significant advantages in the design and development of electrochemical sensors and biosensors. In practice, electrode surface modification has been tried as a means of reducing the overvoltage and overcoming the slow kinetics of many electrode processes [1–4]. A further advantage of chemically modified electrodes is that they are usually less exposed to surface fouling than bare electrodes are. Also, modified electrodes can sometimes separate the electroanalytical signals of solution components whereas, at bare electrode surfaces, the signals appear at potentials close to each other [5–11].

The electrochemical determination of biomolecules has been intensively studied over the past two decades. Noradrenalin (NA) is a very important catecholamine neurotransmitter in the mammalian central nervous system. Many diseases are related to the changes of NA concentration. Thus, the determination of its concentrations in biological systems provides useful information. The determination of NA is usually executed by high-performance liquid chromatography [12–14], gas chromatography [15], ion chromatography [16], capillary electrophoresis [17], and spectrophotometry [18]. NA is also an electroactive compound that can be detected by electrochemical oxidation on various electrodes. The electrochemical oxidation of NA has led to the development of useful methods for measuring NA concentrations [7,19–21].

In addition, acetaminophen (AC) is a widely used analgesic antipyretic drug with actions similar to aspirin. It is a suitable alternative for the patients who are sensitive to aspirin and is safe up to therapeutic doses. Unfortunately, easy availability has resulted in its increased use in attempted suicides. Hence, the need has arisen for the development of rapid and reliable methods for the determination of AC concentration. Many methods have been used for the determination of AC in pharmaceutical formulations and biological fluids including titrimetry [22], UV–vis spectrophotometry [23,24], spectrofluorimetry [25], near infrared transmittance spectroscopy [26], and chromatography [27,28]. Also, electrochemical methods

* Corresponding author. Tel.: +98 351 8122669; fax: +98 351 8210991.
E-mail address: hrzare@yazduni.ac.ir (H.R. Zare).

0039-9140/$ – see front matter © 2009 Elsevier B.V. All rights reserved.
doi:10.1016/j.talanta.2009.07.044

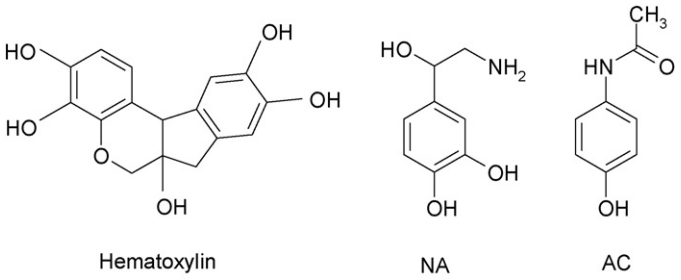

Scheme 1. Structures of hematoxylin, noradrenalin (NA) and acetaminophen (AC).

have attracted much attention because of their quick response, high sensitivity, as well as ability to miniaturize [29–33].

It is known that on a bare electrode, the oxidation peaks of NA and AC are nearly at the same potential, which results in overlapped voltammetric responses making their discrimination highly difficult. Therefore, the establishment of a simple, economical, and accurate analytical method for the simultaneous determination of NA and AC would be useful to medical manufacturers.

Although there are some studies on NA [7,19–21] or AC [29–33] electrochemical oxidation alone, to the best of our knowledge there are no reports about the simultaneous determination of NA and AC using electrochemical or other techniques in the literature. A published paper has reported that AC administrated in high doses results in increased serotonin (5-HT) levels in rat forebrains [34]; 5-HT is known to play a role in NA release in the brain [35]. Also, researchers have investigated the effect of AC and aspirin on the brain [36] and the posterior cortex [37]. The results show that AC administration alone significantly increase NA levels in the forebrain [36] and the posterior cortex [37]. Since so many over-the-counter analgesic preparations contain AC, we decided to investigate the simultaneous determination of NA and AC by electrocatalytic oxidation. Also, there are a few reports concerning the electrocatalytic activity or electrochemical properties of hematoxylin [38–40]. As a follow-up of our studies to prepare modified electrodes for the simultaneous determination of important biological compounds [41–43], we employed a hematoxylin biosensor for NA electrocatalytic oxidation and the simultaneous determination of NA and AC in the physiological pH (pH 7.0). Our findings indicate that a hematoxylin biosensor offers several distinct advantages including extraordinary stability, high surface charge transfer rate constant, and good limit of detection for NA. Differential pulse voltammetry (DPV) was also used to evaluate the analytical performance of the biosensor in quantification of NA in the presence of AC. Finally, to evaluate the utility of the hematoxylin biosensor for analytical applications, it was used for the simultaneous voltammetric determination of NA and AC in real samples.

2. Experimental

2.1. Reagents and apparatus

NA, 4-(2-amino-1-hydroxyethyl)benzene-1,2-diol hydrochloride (see Scheme 1 for structure) was purchased from Aldrich and used without purification. Hematoxylin and AC, 4′-hydroxyacetanilide (see Scheme 1 for their structures) and other reagents were of analytical grade from Merck and used as received. NA injection solution (from Bio&Pharma Companies, Brussels, Belgium), AC oral solution and AC tablet (from Pharma Chemi, Iran) were purchased in a local drugstore. All the solutions were prepared with doubly distilled water. NA and AC solutions were prepared just prior to use.

All the electrochemical experiments were carried out using a potentiostat PGSTAT 30 model from Autolab (Ecochemie, Netherlands), interfaced with a personal computer. The geometrical area of the bare glassy carbon working electrode (Metrohm, Switzerland) was 0.031 cm^2. All the electrochemical experiments were carried out in a conventional three-electrode cell at room temperature. A platinum electrode and a saturated calomel electrode (SCE) were used as the counter and reference electrodes respectively. All the potentials were reported with respect to this reference electrode. pH was measured with a Metrohm model 691 pH/mV meter. Also, the experiments were carried out inside a Faraday cage at room temperature (ca. 25 °C).

2.2. Preparation of the hematoxylin biosensor

The glassy carbon electrode, GCE, was first polished mechanically with 0.05 μm alumina in water slurry using a polishing cloth and then rinsed with doubly distilled water. The electrochemical activation of the electrode was performed by a continuous potential cycling from −1.4 to 1.6 V at a sweep rate of 100 mV s^{-1} in a sodium bicarbonate (0.1 mol L^{-1}) solution until a stable voltammogram was obtained. For modification, the activated electrode was placed in a 0.10 mmol L^{-1} solution of hematoxylin in a 0.15 mol L^{-1} phosphate buffer (pH 7.0), and it was modified by eight cycles of potential sweep between −0.4 and 0.5 V at 50 mV s^{-1}.

3. Results and discussion

3.1. Electrochemical behavior of the hematoxylin biosensor

The mechanism of electrodeposition of *o*- or *p*-hydroquinone derivatives, such as hematoxylin, as modifiers on the surface of an activated GCE has already been discussed [44,45]. Indeed, electrochemical treatment of an electrode surface leads to the formation of some reactive functional groups which can react as nucleophiles with the *o*-quinone produced during the electro-oxidation of the modifier. Fig. 1A shows the cyclic voltammograms of a hematoxylin biosensor in a 0.15 mol L^{-1} phosphate buffer solution (pH 7.0) as the supporting electrolyte at various scan rates. When the potential was scanned between −30 and 300 mV, a surface immobilized redox couple with a formal potential ($E^{0'}$) value of 104 mV was observed. In addition, the formal potential, $E^{0'}$, was almost independent of the potential scan rate for sweep rates ranging from 10 mV to 2000 mV s^{-1}, suggesting facile charge transfer kinetics over this range of sweep rate. The peak-to-peak potential separation ($\Delta E_p = E_{pa} - E_{pc}$) was small, and about 70 mV for the sweep rates below 1000 mV s^{-1}. Also, the electrochemical responses of the biosensor were those anticipated for a surface-confined redox couple because the anodic and cathodic peak currents were directly proportional to the scan rate (not shown), as predicted for the deposited chemical species at the electrode surface. The ratio of cathodic to anodic peak currents at various scan rates was almost constant. The electron transfer coefficient, α, between the electrode and the surface-confined redox couple can be evaluated in cyclic voltammetry from the variation of the anodic and cathodic peak potentials with the logarithm of scan rates, according to the method described by Laviron [46]. For high scan rates, this theory predicts a linear dependence of E_p upon $\log \nu$, which can be used to extract the kinetic parameter of α from the slope of such plots. We found that for the scan rates above 3 V s^{-1} the value of E_{pa} and E_{pc} were proportional to the $\log \nu$ (Fig. 1B). Using these plots at pH = 7.0, the value of $\alpha = 0.59$ was obtained.

3.2. Electrocatalytic oxidation of NA at the hematoxylin biosensor

The cyclic voltammetric responses of the bare GCE in a 0.15 mol L^{-1} phosphate buffer (pH 7.0), without and with NA in solution, are shown in Fig. 2 (curves c and d respectively). If a

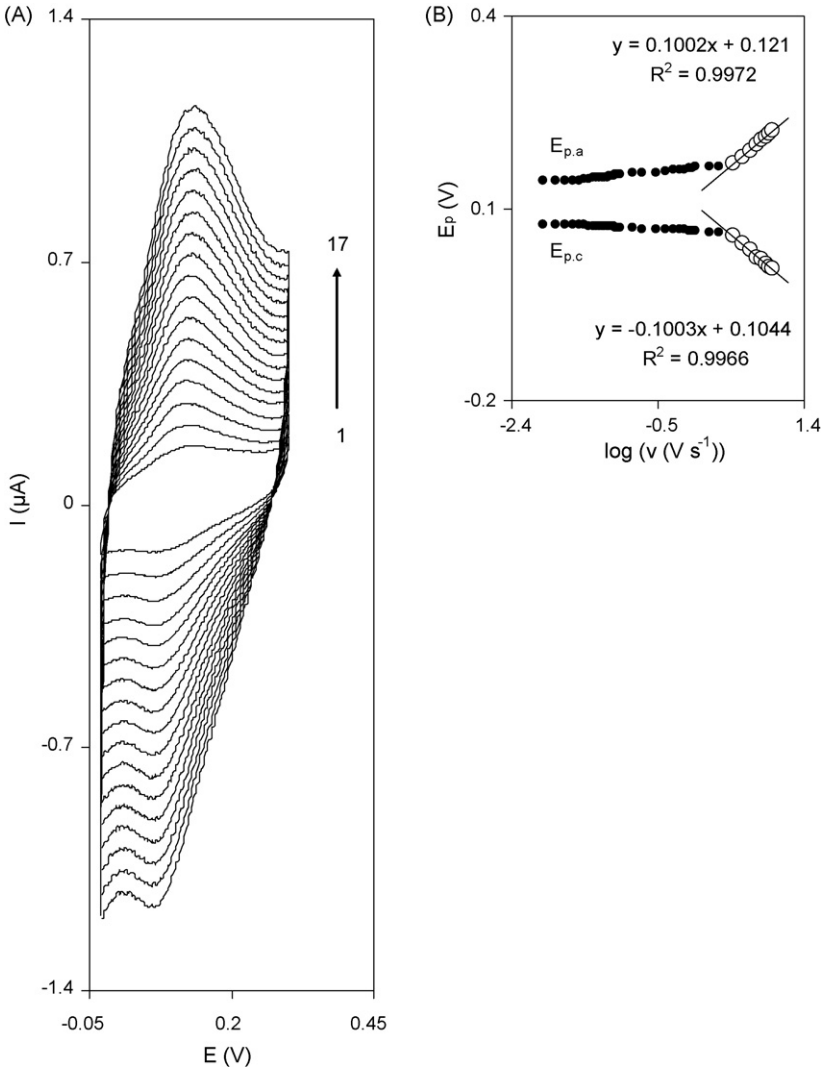

Fig. 1. (A) Cyclic voltammograms of the hematoxylin biosensor in a 0.15 mol L^{-1} phosphate buffer (pH 7.0) at various scan rates. The numbers 1–17 correspond to 10, 15, 20, 25, 30, 35, 40, 45, 50, 55, 60, 65, 70, 75, 80, 85 and 90 mV s^{-1}, respectively. (B) Variation of E_p versus the logarithm of the scan rate.

hematoxylin biosensor is placed into the same NA containing an electrochemical cell, a large anodic peak is observed without a cathodic counterpart (Fig. 2, curve b). That the current observed is associated with the NA oxidation and not only with the oxidation of surface-attached hematoxylin is demonstrated by comparing the current in curve b with that in curve a. Fig. 2, curve a, shows the cyclic voltammetric behavior of the hematoxylin biosensor in a NA-free electrolyte (0.15 mol L^{-1} phosphate buffer with pH 7.0). It is apparent that the anodic current associated with the surface-attached materials is significantly lower than that obtained in the solution containing NA. The anodic peak potential for the oxidation of NA at the hematoxylin biosensor is about 150 mV (Fig. 2, curve b), while NA starts to oxidize at about 570 mV (Fig. 2, curve d) at the bare GCE under identical conditions. So, a decrease in an overpotential of about 420 mV is observed.

The cyclic voltammograms of the hematoxylin biosensor at various scan rates obtained in a 0.15 mol L^{-1} phosphate buffer solution (pH 7.0) containing 0.25 mmol L^{-1} NA are shown in Fig. 3A. As shown in Fig. 3A inset, curve a, the oxidation currents increase linearly with the square root of the scan rate, suggesting that at a sufficient overpotential the reaction is mass transport controlled. From the slope of the I_P versus $v^{1/2}$ plot can be obtained the number of electrons in the overall reaction. According to the following equation for a totally irreversible diffusion controlled processes [47]:

$$I_p = 3.01 \times 10^5 n[(1-\alpha)n_\alpha]^{1/2} A C_b D^{1/2} v^{1/2} \quad (1)$$

and considering $(1-\alpha)n_\alpha = 0.69$ (see below), $D = 5.8 \times 10^{-6}$ cm^2 s^{-1} (D was determined by chronoamperometry), and $A = 0.0314$ cm^2, it is estimated that the total number of electrons involved in the anodic oxidation of NA is $n = 2.1 \cong 2$. Also, the plot of the scan rate-normalized current ($I_p/v^{1/2}$) versus the scan rate (Fig. 3A inset, curve b) exhibits a characteristic shape typical of an EC_{cat} process. These results show that the overall electrochemical oxidation of NA at the biosensor might be controlled by the cross exchange process between the redox site of the hematoxylin and the diffusion of NA. Under these conditions for EC catalytic mechanism, Andrieux and Saveant theoretical model [48] can be used to calculate the catalytic rate constant between NA and hematoxylin, k'. According to the approach of Andrieux and Saveant and using Fig. 1 in their theoretical paper [48], the average value of k' was calculated to be $(3.64 \pm 0.49) \times 10^{-3}$ cm s^{-1}.

The inset of Fig. 3B shows a Tafel plot that was drawn from the data of the rising part of the current–voltage curve recorded at a scan rate of 30 mV s^{-1} (Fig. 3B). This part of voltammogram, known as Tafel region, is affected by the electron transfer kinetics between the substrate (NA) and the surface-confined hematoxylin,

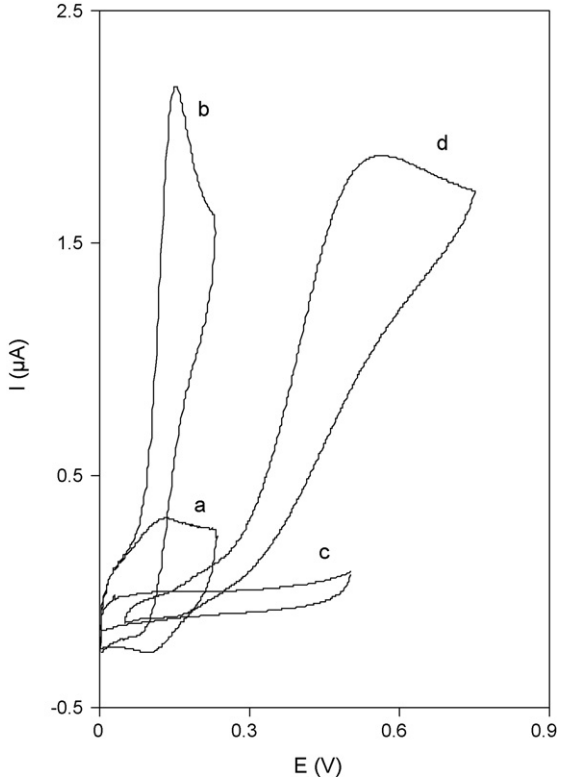

Fig. 2. Cyclic voltammograms of the hematoxylin biosensor in a 0.15 mol L^{-1} phosphate buffer (pH 7.0) solution in the absence (a) and presence (b) of 0.15 mmol L^{-1} NA. (c) As (a) and (d) as (b) for a bare GCE. In all cases the scan rate was 20 mV s^{-1}.

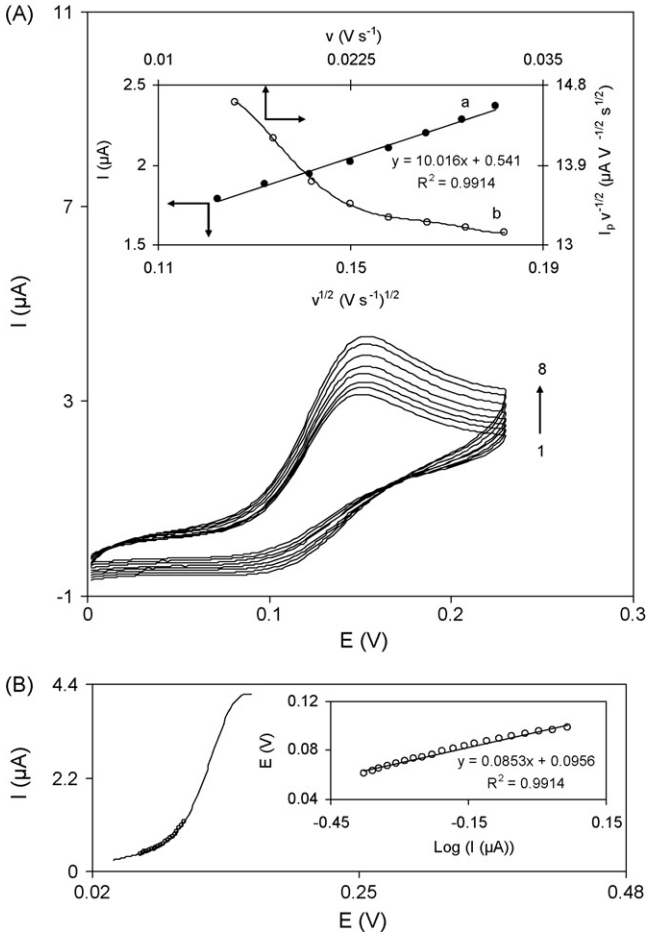

Fig. 3. (A) Cyclic voltammograms of the hematoxylin biosensor in a 0.15 mol L^{-1} phosphate buffer (pH 7.0) containing 0.25 mmol L^{-1} NA at different scan rates. The numbers of 1–8 correspond to 15, 17.5, 20, 22.5, 25, 27.5, 30 and 32.5 mV s^{-1}, respectively. Inset shows the plot (a) variation of the electrocatalytic peak current (I_p) with the square root of sweep rate and (b) variation of the sweep rate-normalized current ($I_p/v^{-1/2}$) with the sweep rate. (B) Linear sweep voltammogram recorded at 30 mV s^{-1}. Inset shows the Tafel plot derived from the linear sweep voltammogram.

assuming the deprotonation of the substrate as a sufficiently fast step. In this condition, the number of electrons involved in the rate-determining step can be estimated from the slope of Tafel plot. A slope 0.0853 V decade^{-1} is obtained indicating a one-electron transfer in the rate-determining step of the electron transfer process, assuming a charge transfer coefficient of $\alpha = 0.31$ [49].

The catalytic oxidation of NA with a hematoxylin biosensor was also studied by chronoamperometry. The chronoamperometric measurements of different concentrations of NA at a biosensor were done by setting the working electrode potential at 200 mV. In chronoamperometric studies, based on Cottrell equation [49], we have determined the diffusion coefficient of NA. Fig. 4A shows the experimental plots of I verses $t^{-1/2}$ with the best fit for different concentrations of NA employed. The slopes of the resulting straight line were then plotted versus the NA concentration (Fig. 4B), from whose slope we calculated a diffusion coefficient of 5.8×10^{-6} cm^2 s^{-1} for NA.

In order to elucidate the kinetics of NA oxidation at a hematoxylin biosensor, RDE measurements were performed at different rotation speeds in a 0.15 M phosphate buffer (pH 7.0) containing various concentrations of NA. Fig. 5 represents a typical example of RDE voltammograms of a 0.50 mmol L^{-1} NA at the biosensor as a function of the electrode rotation rates. Levich plots obtained at 220 mV for different concentrations of NA are shown in Fig. 5, inset A. According to Levich plots, the current increases with increasing electrode rotation speed but was found to be nonlinear. The clear lack of linearity immediately suggests that the reaction is limited by kinetics and not by transport [49]. In addition, we again conclude that the reaction between NA and the electrodeposited hematoxylin is the sole rate-limiting step [50]. In such cases, the currents are conveniently analyzed by plots of I^{-1} versus $\omega^{-1/2}$ [49]. Fig. 5, inset B, presents such plots (so-called Koutecky–Levich plots) and, in this case, well behaved linear responses are obtained. The value of catalytic reaction rate constant, k', between the oxidized form of the deposited hematoxylin and NA can be calculated from the intercepts of Koutecky–Levich plots [49]. From the values of the intercept of various plots, the mean values of k' dependent on potentials of 140, 160, 180, 200, and 220 mV are calculated and the results are shown in Table 1. As it can be seen in Fig. 5, inset C, and Table 1, the rate constant, k', is strongly potential dependent and k' increases with the increase of the potential which is considered for obtaining Koutecky–Levich plots. The kinetic parameters of the standard heterogeneous rate constant, k^0, and transfer coefficient, α, can be evaluated from the intercept and the slope of the plot of $\ln k'$ versus $E - E^{0'}$ (Fig. 5, inset C), according to the following equation described in [49]:

$$k'(E) = k' = k^0 \exp\left[\frac{n_\alpha(1-\alpha)F(E-E^{0'})}{RT}\right] \quad (2)$$

where E and $E^{0'}$ are the potentials which are considered for the obtained Koutecky–Levich plot and the formal potential of

Table 1
The relationship between the heterogeneous electron transfer rate constant, k', and the considered potential, E, in drawing the Koutecky–Levich plots.

E (mV)	140	160	180	200	220
$\times 10^3\, k'$ (cm s^{-1})	2.79	4.65	7.71	14.10	24.2

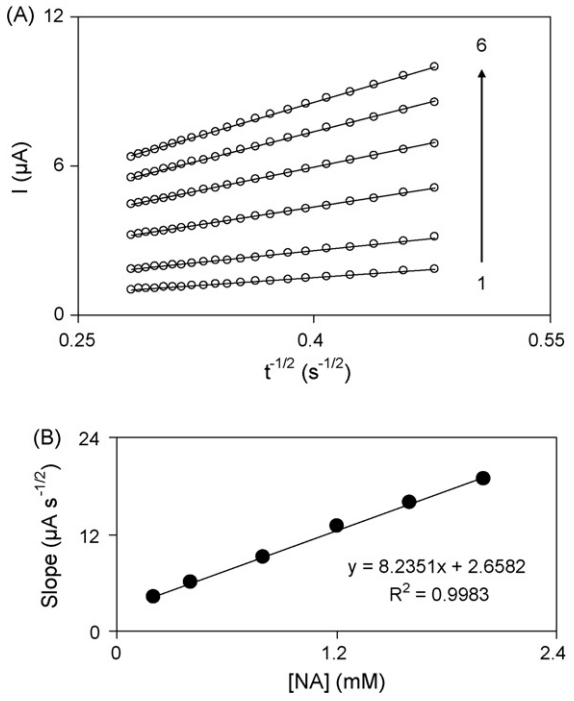

Fig. 4. (A) Plots of I versus $t^{-1/2}$ obtained from chronoamperometric experiments for the hematoxylin biosensor in a 0.15 mol L^{-1} phosphate buffer (pH 7.0) at a potential step 200 mV for different concentrations of NA. The numbers of 1–6 correspond to 0.20, 0.40, 0.80, 1.20, 1.60 and 2.00 mmol L^{-1} of NA. (B) Plot of the slope of straight lines against the NA concentration.

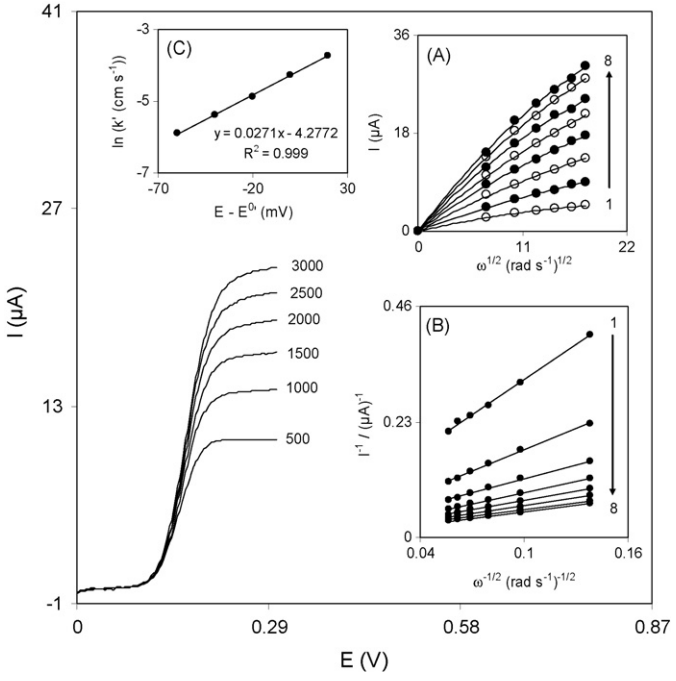

Fig. 5. Voltammograms of a rotating disk hematoxylin biosensor in a 0.15 M phosphate buffer (pH 7.0) containing 0.50 mmol L^{-1} NA at the various rotation rates indicated for each voltammograms. Insets: (A) Levich plots constructed from the modified RDE voltammograms and using current for E_{disk} = 220 mV of different concentrations of NA. The numbers of 1–8 correspond to 0.10, 0.20, 0.30, 0.40, 0.50, 0.60, 0.70 and 0.80 mmol L^{-1} of NA. (B) Koutecky–Levich plots obtained from Levich plots shown in inset (A). (C) Plot of the ln k' versus the $E - E^{0'}$. E and $E^{0'}$ are the potentials which were considered for obtaining the Koutecky–Levich plot and the formal potential of hematoxylin.

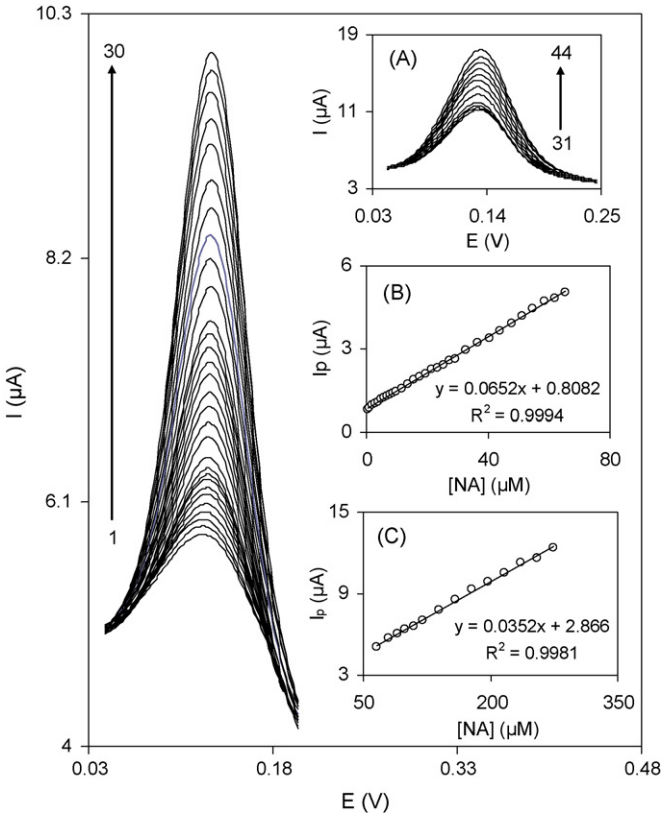

Fig. 6. Differential pulse voltammograms of the hematoxylin biosensor in a 0.15 mol L^{-1} phosphate buffer solution (pH 7.0) containing different concentrations of NA. The numbers of 1–30 correspond to 5.0×10^{-1} to 65.40 μmol L^{-1} of NA. Insets: (A) DPVs of the hematoxylin biosensor in solution containing 65.40–274.20 μmol L^{-1} of NA. (B) and (C) shows the plots of the electrocatalytic peak current as a function of NA concentration in the range of 5.0×10^{-1} to 65.40 and 65.40–274.20 μmol L^{-1} of NA, respectively.

hematoxylin respectively. The slope of 0.0271 mV^{-1} was obtained, indicating that a one-electron process is involved in the rate-determining step, $n_\alpha = 1$, assuming a charge transfer coefficient of $\alpha = 0.30$. This value of α is very close to that obtained from Tafel plot previously discussed. Also, the value of k^0 is found to be 1.02×10^{-3} cm s^{-1} from the intercept of Fig. 5, inset C. The value obtained for k^0 indicates that the electron transfer between the electrodeposited hematoxylin and NA is fast enough. Thus, hematoxylin can be used as a good electron transfer mediator for NA electrocatalytic oxidation.

3.3. Differential pulse voltammetric detection of NA and AC at the hematoxylin biosensor

The main objective in this study was the development of a biosensor capable of the electrocatalytic oxidation of NA and simultaneous detection of NA and AC. Since differential pulse voltammetry (DPV) has a much higher current sensitivity than cyclic voltammetry, it was used to estimate the lower limit of detection and the linear range of NA. In addition, the charging current contribution to the background current, which is a limiting factor in the analytical determination, is lower in DPV mode. The effects of increasing the concentration of NA on the voltammograms are presented in Fig. 6 (in range of 5.0×10^{-1} to 65.40 μmol L^{-1}) and its inset A (in range of 65.40–274.20 μmol L^{-1}). Also, insets B and C of Fig. 6 clearly show that the plot of the peak current versus the NA concentration is constituted of two linear segments (5.0×10^{-1} to 65.40 μmol L^{-1} and 65.40–274.20 μmol L^{-1}) with different slopes.

Table 2
Comparison of analytical parameters of several biosensors for NA determination.

Modifier	Method[a]	Linear range (μmol L^{-1})	Detection limit (μmol L^{-1})	Refs.
Polycalconcarboxylic acid	DPV	0.63–62.50	0.1	[7]
Poly(isonicotinic acid)	DPV	0.40–10.00 10.0–200.0	0.006	[20]
Tetrakis-(2-aminopheny) porphyrin	CV	1.0–7.0 7.0–50.0	–	[21]
C60-[dimethyl-(b-cyclodextrin)]$_2$	CV	50.0–800.0	8.0	[46]
β-Cyclodextrin	CV	1.0–300.0	0.50	[47]
Hematoxylin	DPV	0.50–65.40 65.40–274.20	0.14	This work

[a] DPV: differential pulse voltammetry, CV: cyclic voltammetry.

The plot of the average peak current of three replicates of DPVs versus NA concentration in the range of 5.0×10^{-1} to 4.00 μmol L^{-1} (not shown) was used to estimate the lower limit of NA detection at the biosensor. For these low concentrations, a linear correlation with a slope of 0.0673 μA μmol^{-1} L and a correlation coefficient 0.9943 are observed between the measured average current and the NA concentration. From the analysis of these data, we estimate that the lower limit of detection ($X_{\text{l.o.d.}}$) of NA is 0.14 μmol L^{-1} according to the definition $X_{\text{l.o.d.}} = (Y_{\text{l.o.d.}} - Y_{\text{bl.}})/m$ [51]. The lower detection limit of NA obtained in this method is lower than those previously reported for other biosensors [17,52–54]. The average voltammetric peak current and the precision estimated in terms of the coefficient of variation for 16 repeated measurements ($n = 16$) of 5.00 μmol L^{-1} NA at the hematoxylin biosensor were 1.13 ± 0.03 μA and 2.6% respectively. The coefficient of variation value indicates that the biosensor is stable and does not undergo surface fouling during the voltammetric measurements. This also demonstrates the fact that the results obtained at the biosensor are reproducible in analytical applications. In Table 2, some of the response characteristics obtained in this work are compared with those previously reported by others [7,20,21,52,53]. These data show that the responses of the proposed biosensor are superior in most cases to those of the previously reported biosensors.

The next attempt was made to detect NA and AC simultaneously by using a hematoxylin biosensor. Fig. 7 shows the differential pulse voltammetric responses which were gained by varying either the NA (Fig. 7A) or AC (Fig. 7B) concentration while the concentration of the other compound was kept constant. As shown in Fig. 7A, the electrochemical response of NA in the presence of a constant concentration of 5.0×10^{-1} mmol L^{-1} AC increased linearly with the increase of the NA concentration, while the response of AC remaining almost constant. Similarly, Fig. 7B shows DPVs obtained by increasing the concentrations of AC in the presence of 2.0×10^{-1} mmol L^{-1} NA. As it can be seen, an increase in the peak current of AC is observed with increasing AC concentration, while the voltammetric peak of NA is almost unchanged during the oxidation of AC. It can also be noted from these results that the responses to NA and AC at the biosensor are relatively independent. On the other hand, Fig. 7C shows the DPV of a mixture of 1.0×10^{-1} mmol L^{-1} NA and 4.0×10^{-1} mmol L^{-1} AC at the bare GCE. As shown, the bare GCE could not separate the voltammetric signals of NA–AC, and only one broad voltammetric signal at around 304 mV was obtained.

The utilization of the hematoxylin biosensor for the simultaneous determination of NA and AC was demonstrated by simultaneously changing the concentrations of NA and AC. The DP voltammetric results show that the simultaneous determination of NA and AC with two well distinguished anodic peaks at potentials of 127 and 300 mV, corresponding to the oxidation of NA and AC, is possible at the biosensor (Fig. 8). Fig. 8, inset A, shows that the linear range of NA concentration is 7.5×10^{-1} to 65.40 μmol L^{-1}. Also insets B and C of Fig. 8 clearly show that the plot of the peak current versus the AC concentration is constituted of two linear segments of 12.00–59.10 μmol L^{-1} and 59.10–261.70 μmol L^{-1} with different slopes, corresponding to two different ranges of substrate concentration. The decrease of sensitivity (slope) in the second linear range (Fig. 8, inset C) is likely to be due to kinetic limitation. Comparing Fig. 6, inset B, to Fig. 8, inset A, the sensitivities to NA in the absence and presence of AC were found to be 0.0652 (absence of AC) and 0.0697 (presence of AC) μA μmol^{-1} L. It is very interesting to note that the sensitivities of the biosensor to NA in the absence and presence of AC are virtually the same, which indicates the fact that the oxidation processes of NA at the hematoxylin biosensor are independent and, therefore, simultaneous or independent measurements of the two analytes are possible without any interference. If the NA signal was affected by AC, the above-mentioned slopes would be different.

Table 3
Determination of NA and AC in pharmaceutical formulations using calibration plots and with the hematoxylin biosensor[a].

Samples	Added (μmol L^{-1})		Found[a] (μmol L^{-1})		RSD (%)		Recovery (%)	
	NA	AC	NA	AC	NA	AC	NA	AC
Injection solution of NA	–	–	4.74	–	2.8	–	–	–
	5.00	40.00	9.99	38.63	1.2	1.6	103	97
	10.00	50.00	14.60	51.10	1.7	2.0	99	102
Oral solution of AC	–	–	–	15.46	–	3.0	–	–
	8.00	15.00	8.08	31.32	2.3	2.0	101	103
	12.00	30.00	12.39	46.22	1.5	1.8	103	102
Tablet of AC	–	–	–	20.88	–	3.0	–	–
	10.00	20.00	9.79	42.16	1.9	1.0	98	103
	15.00	40.00	14.83	61.67	2.1	2.0	99	101

[a] Three replicate measurements were made on the same samples.

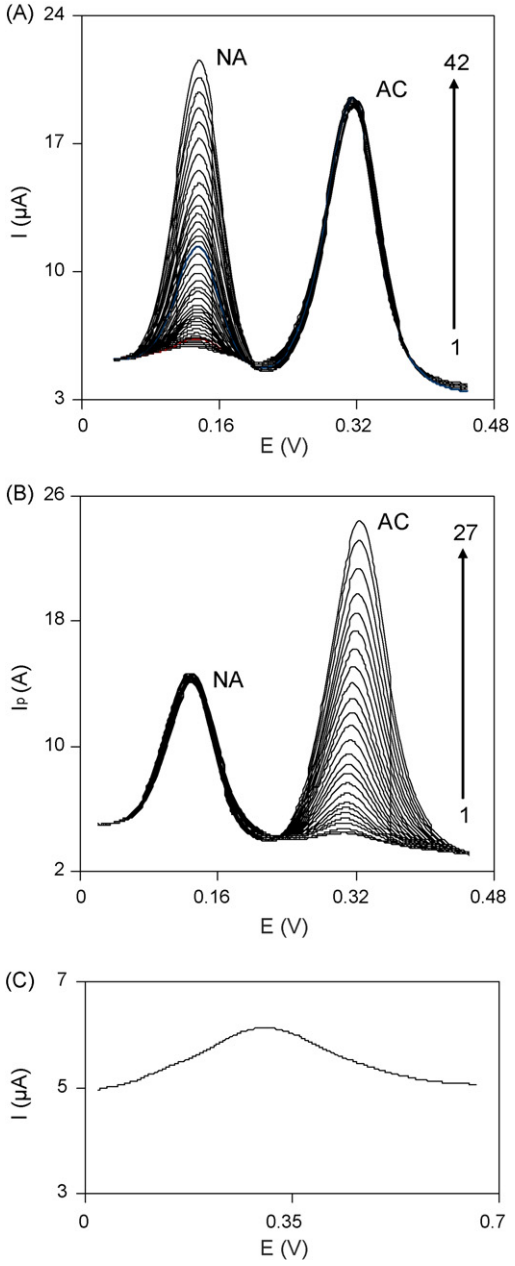

Fig. 7. (A) Differential pulse voltammograms of the hematoxylin biosensor in a 0.15 mol L^{-1} phosphate buffer solution (pH 7.0) containing 5.0×10^{-1} mmol L^{-1} AC and different concentrations of 5.0×10^{-1} to 488.00 μmol L^{-1} of NA. (B) Differential pulse voltammograms of the hematoxylin biosensor in a 0.15 mol L^{-1} phosphate buffer solution (pH 7.0) containing 2.0×10^{-1} mmol L^{-1} of NA and different concentrations of 12.00–1150.00 μmol L^{-1} of AC. (C) Shows the response at a bare GCE for the oxidation of a mixed solution of 1.0×10^{-1} mmol L^{-1} of NA and 4.0×10^{-1} μmol L^{-1} of AC.

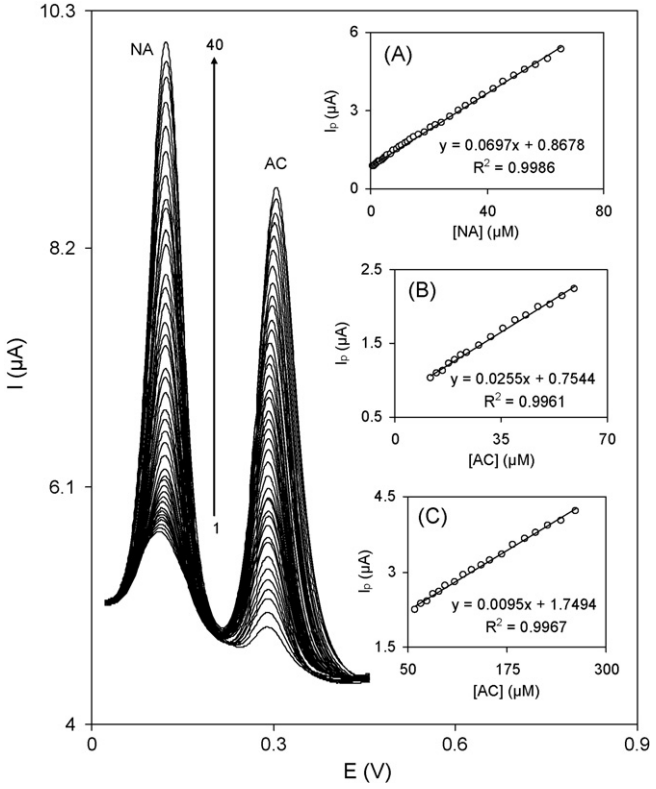

Fig. 8. Differential pulse voltammograms of the hematoxylin biosensor in a 0.15 mol L^{-1} phosphate buffer solution (pH 7.0) in mixed solutions of (from inner to outer): 7.5×10^{-1} to 65.40 μmol L^{-1} for NA and 12.00–261.70 μmol L^{-1} for AC. Insets: (A) plot of the peak currents as a function of NA concentration in the linear range of 7.5×10^{-1} to 65.40 μmol L^{-1}. (B) and (C) Plots of the peak currents as a function of concentration of AC in two linear ranges of 12.00–59.10 and 59.10–261.70 μmol L^{-1}.

3.4. Application of the hematoxylin biosensor for determination of NA and AC in real samples

The utility of the present hematoxylin biosensor for determination of NA and AC in pharmaceutical formulations was tested by measuring the NA concentration in an injection solution and the AC concentration in an oral solution and tablet samples. The NA injection solution and the AC oral solution were diluted 10^3 and 10^4 times respectively. Also one tablet of AC (0.4356 g), after dissolving in 1 L doubly distilled water was diluted 100 times with a phosphate buffer solution before the measurements. The differential pulse voltammograms of various real samples solutions are shown in curve (a) Fig. 9A–C. The measurements were performed using the calibration plots which are shown in Fig. 8, insets, and the results obtained are listed in Table 3. To authenticate the validity of the results, the samples were spiked with certain amounts of NA and AC at levels similar to those found in the samples themselves. The results in Table 3 show that the relative standard deviations (RSD%) and the recovery rates of the spiked samples were acceptable. Thus, the proposed biosensor can be efficiently used for the simultaneous determination of NA and AC in pharmaceutical samples. The reliability of the proposed biosensor was also evaluated by comparing the obtained results with those declared in the label of the pharmaceutical inhalation products. The data in Table 4 demonstrate that the results obtained by a differential pulse voltammetric method (utilizing the biosensor) are in very good agreement with the values declared in the label of the analytes.

Table 4
Comparison of the total values of NA and AC of various formulations obtained using the hematoxylin biosensor with those declared in the label of the pharmaceutical inhalation products[a].

Samples	Declared value	Found value	RSD (%)
Injection solution of NA (mg mL^{-1})	1.0	0.98	3.1
Oral solution of AC (mg mL^{-1})	24.0	23.37	3.0
Tablet of AC (mg g^{-1})	725.3	724.62	2.9

[a] The total values (average of three measurements) were obtained by multiplying the measured values by the appropriate dilution factor and number of sample assayed was three.

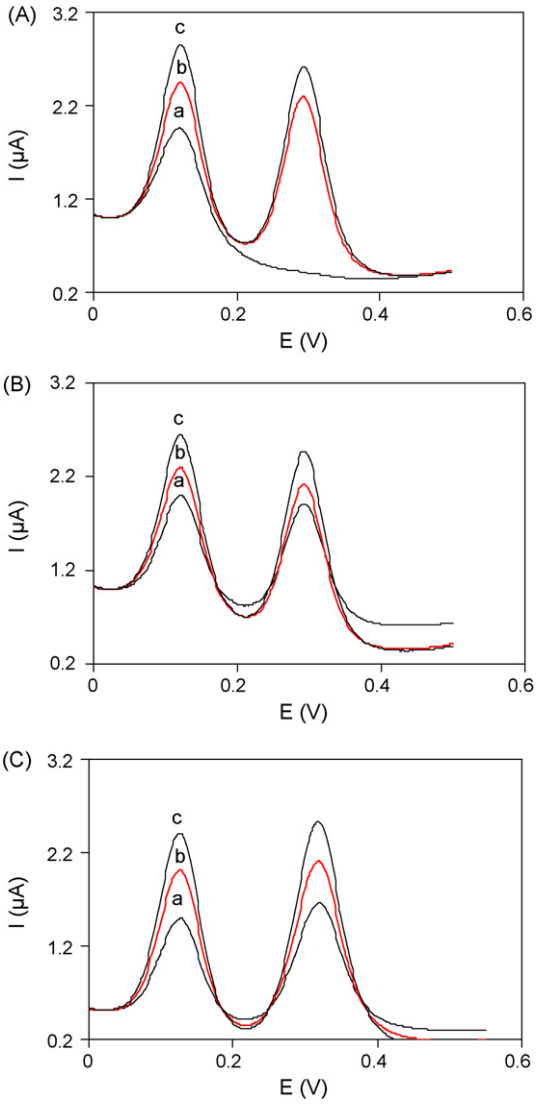

Fig. 9. Voltammograms of (a) are shown the differential pulse voltammograms of the hematoxylin biosensor in a 0.15 mol L^{-1} phosphate buffer solution (pH 7.0) containing a concentration of the real samples which indicated in Table 3 for (A) an NA injection solution, (B) AC oral solution and (C) AC tablet. In all cases, for voltammograms of (b) and (c), different concentrations of NA and AC added to the real samples according to the data which reported in Table 3.

4. Conclusions

In this study, a simple and fast procedure was used for the electrodeposition of hematoxylin on a GCE. The electrodeposited hematoxylin layers on the GCE exhibited excellent electrocatalytic activity toward the electro-oxidation of NA, which appeared as a reduced overpotential and an increase in the peak current. The transfer coefficient, α, the catalytic rate constant, k', the standard catalytic rate constant, k^0, and the overall number of electrons involved in the electrocatalytic oxidation of NA at a hematoxylin biosensor surface were determined using voltammetric methods. The diffusion coefficient of NA was calculated as 5.8×10^{-6} cm^2 s^{-1} for experimental conditions, using chronoamperometric results. The hematoxylin biosensor could successfully separate the voltammetric peaks of NA and AC, which are indistinguishable on a bare GCE. The precision of the differential pulse voltammetry (DPV) method was found to be 2.6% for the replicate determination of a 5.00 μmol L^{-1} solution of NA ($n = 16$). Also, in DPV measurements, two linear calibration ranges were obtained for NA and AC. The sensitivities of NA and AC determination at the biosensor surface were obtained 0.0697 and 0.0255 μA μmol^{-1} L respectively. The proposed hematoxylin biosensor has been applied to the simultaneous determination of NA and AC in an injection solution of NA, an oral solution of AC, and a tablet of AC with satisfactory results. Thus, the reliability and stability of the biosensor offers a good possibility for applying the technique to a routine analysis of NA and AC in pharmaceutical formulations.

References

[1] A. Salimi, A. Noorbakhsh, M. Ghadermarzi, Sen. Actuators B 123 (2007) 530.
[2] S.M. Golabi, H.R. Zare, M. Hamzehloo, Electroanalysis 14 (2002) 611.
[3] H.R. Zare, Z. Sobhani, M. Mazloum-Ardakani, Sen. Actuators B 126 (2007) 641.
[4] H.R. Zare, N. Nasirizadeh, Electroanalysis 18 (2006) 507.
[5] J. Huang, Y. Liu, H. Hou, T. You, Biosens. Bioelectron. 24 (2008) 632.
[6] J.M. Zen, C.T. Hsu, Y.L. Hsu, J.W. Sue, E.D. Conte, Anal. Chem. 76 (2004) 4251.
[7] A.L. Liu, S.B. Zhang, W. Chen, X.H. Lin, X.H. Xia, Biosens. Bioelectron. 23 (2008) 1488.
[8] H.R. Zare, N. Rajabzadeh, N. Nasirizadeh, M. Mazloum-Ardakani, J. Electroanal. Chem. 589 (2006) 60.
[9] J. Li, X.-Q. Lin, Anal. Chim. Acta 596 (2007) 222.
[10] G. Hu, Y. Ma, Y. Guo, S. Shao, Electrochim. Acta 53 (2008) 6610.
[11] L. Lin, J. Chen, H. Yao, Y. Chen, Y. Zheng, X. Lin, Bioelectrochemistry 73 (2008) 11.
[12] V. Carrera, E. Sabater, E. Vilanova, M.A. Sogorb, J. Chromatogr. B 847 (2007) 88.
[13] H. Wang, H. Jin, H.S. Zhang, Fresenius J. Anal. Chem. 365 (1999) 682.
[14] N. Aoyama, M. Tsunoda, K. Imai, J. Chromatogr. A 1074 (2005) 47.
[15] D.L. Kuhlenbeck, T.P.O. Neill, C.E. Mack, S.H. Hoke, K.R. Wehmeyer, J. Chromatogr. B 738 (2000) 319.
[16] C.L. Guan, J. Quyang, Q.L. Li, B.H. Liu, W.R.G. Baeyens, Talanta 50 (2000) 1197.
[17] S. Wei, G. Song, J.M. Lin, J. Chromatogr. A 1098 (2005) 166.
[18] M. Zhu, X.M. Huang, J. Li, H.X. Shen, Anal. Chim. Acta 357 (1997) 261.
[19] G. Wang, X. Liu, B. Yu, G. Luo, J. Electroanal. Chem. 567 (2004) 227–231.
[20] H. Zhao, Y. Zhang, Z. Yuan, Anal. Chim. Acta 454 (2002) 75.
[21] H. Jeong, H. Kim, S. Jeon, Microchem. J. 78 (2004) 181.
[22] K.G. Kumar, R. Letha, J. Pharm. Biomed. Anal. 15 (1997) 1725.
[23] V. Rodenas, M.S. Garcia, C. Sanchez-Pedreno, M.I. Albero, Talanta 52 (2000) 517.
[24] N. Erk, Y. Ozkan, E. Banoglu, S.A. Ozkan, Z. Senturk, J. Pharm. Biomed. Anal. 24 (2001) 469.
[25] J.L. Vilchez, R. Blanc, R. Avidad, A. Navalon, J. Pharm. Biomed. Anal. 13 (1995) 1119.
[26] A. Eustaquio, M. Blanco, R.D. Jee, A.C. Moffat, Anal. Chim. Acta 383 (1999) 283.
[27] J.L. Perez, M.A. Bello, Talanta 48 (1999) 1199.
[28] D.J. Speed, S.J. Dickson, E.R. Cairns, N.D. Kim, J. Anal. Toxicol. 25 (2001) 198.
[29] M. Li, L. Jing, Electrochim. Acta 52 (2007) 3250.
[30] F.S. Felix, C.M.A. Brett, L. Angnes, J. Pharm. Biomed. Anal. 43 (2007) 1622.
[31] S.F. Wang, F. Xie, R.F. Hu, Sens. Actuators B 123 (2007) 495.
[32] M.L.S. Silva, M.B.Q. Garcia, J.L.F.C. Lima, E. Barrado, Anal. Chim. Acta 573 (2006) 383.
[33] M. Boopathi, M.S. Won, Y.B. Shim, Anal. Chim. Acta 512 (2004) 191.
[34] S. Daya, S. Anoopkumar-Dukie, Life Sci. 67 (2000) 235.
[35] S.L. Xi-Ming, K.W. Perry, D.T. Wong, Neuropharmacology 42 (2002) 181.
[36] H. Maharaj, D.S. Maharaj, K.S. Saravanan, K.P. Mohanakumar, S. Daya, Metabol. Brain Dis. 19 (2004) 71.
[37] Naunyn-Schmiedeberg's Arch. Pharmacol. 364 (2001) 534.
[38] H.R. Zare, N. Nasirizadeh, M. Mazloum-Ardakani, M. Namazian, Sens. Actuators B 120 (2006) 288.
[39] H.R. Zare, N. Nasirizadeh, Electrochim. Acta 52 (2007) 4153.
[40] A.M.H. El-Askalany, A.M.A. El-Magd, Chem. Pharm. Bull. 43 (1995) 1791.
[41] H.R. Zare, F. Memarzadeh, M. Mazloum-Ardakani, M. Namazian, S.M. Golabi, Electrochim. Acta 50 (2005) 3495.
[42] H.R. Zare, N. Nasirizadeh, S.M. Golabi, M. Namazian, M. Mazloum-Ardakani, D. Nematollahi, Sens. Actuators B 114 (2006) 610.
[43] H.R. Zare, N. Nasirizadeh, M. Mazloum-Ardakani, J. Electroanal. Chem. 577 (2005) 25.
[44] F. Pariente, F. Tobalina, M. Darder, E. Lorenzo, H.D. Abruna, Anal. Chem. 68 (1996) 3135.
[45] H.R. Zare, S.M. Golabi, J. Electroanal. Chem. 464 (1999) 14.
[46] E. Laviron, J. Electroanal. Chem. 101 (1979) 19.
[47] S. Antoniadou, A.D. Jannakoudakis, E. Theodoridou, Synth. Met. 30 (1989) 295.
[48] C.P. Andrieux, J.M. Saveant, J. Electroanal. Chem. 93 (1978) 163.
[49] A.J. Bard, L.R. Faulkner, Electrochemical Methods, Fundamentals and Applications, Wiley, New York, 2001.
[50] R.D. Rocklin, R.W. Murray, J. Phys. Chem. 85 (1981) 2104.
[51] J.N. Miller, J.C. Miller, Statistics and Chemometrics for Analytical Chemistry, 4 ed., Pearson Education Ltd., Harlow, UK, 2000.
[52] M. Wei, M. Li, N. Li, Z. Gu, X. Duan, Electrochim. Acta 47 (2002) 2673.
[53] G. Wang, X. Liu, B. Yu, G. Luo, J. Electroanal. Chem. 567 (2004) 227.
[54] Y. Baoxian, X. Ping, L. Lin, Microchem. J. 64 (2000) 125.